Perturbation theory for surface-profile imaging with a capacitive probe

A. García-Valenzuela,[a] N. C. Bruce, and D. Kouznetsov
Laboratorio de Optica Aplicada, Centro de Instrumentos, Universidad Nacional Autónoma de México, Circuito Exterior C.U., A.P. 70-186, México D.F. 04510, México

(Received 2 June 2000; accepted for publication 28 July 2000)

We derive a perturbative series solution to the capacitance between two parallel electrodes with irregular profiles. The coefficients in the series are calculated using fast Fourier transform algorithms resulting in a very fast method. The applicability of the perturbative series solution is extended by introducing a spectral window function which can make the series converge in cases where the standard series does not converge. We show that the filtered perturbative solution is applicable to surface profiles with surprisingly large features. However, limitations on its applicability to surfaces with high spatial frequencies remain. Perturbation theory could be a powerful tool for simulating surface-profile images obtained by scanning a capacitive probe. © *2000 American Institute of Physics*. [S0003-6951(00)02539-0]

The capacitance between two parallel electrodes with irregular profiles can be approximated in some cases by a simple ''local height approximation.'' [1–3] However, if the surface profiles are not smooth or have a large amplitude compared to the mean distance between electrodes the approximation will not generally be valid. A more accurate calculation of the surface charges on the electrodes is needed. Most numerical methods are very time consuming. Recently, perturbation techniques to solve the boundary integral equations for the surface charge between two electrodes where one electrode has a rough profile have been investigated.[2–5] An important advantage of perturbation theory (PT) is the speed of evaluation. Each term of the series involve Fourier transforms which can be evaluated very fast using fast Fourier transform (FFT) algorithms. In particular, scanning capacitance microscopy and related techniques have been used for some time now.[6–9] In this letter we report on the possible application of PT to simulate surface profile images obtained by scanning a capacitance probe.

Let us consider the electrode geometry depicted in Fig. 1. The lower electrode's profile is given by $y=h_b(x,z)$ and the upper electrode's profile by $y=D+h_a(x,z)$, where D is the separation between the corresponding flat electrodes. We will first derive the perturbative series in the usual way.Consider the boundary integral equation[2]

$$\int_{-\infty}^{\infty}\left(U_b\frac{\partial G}{\partial N_b}-G\frac{\partial\phi}{\partial N_b}\right)\Bigg|_{y=h_b}dxdz + \int_{-\infty}^{\infty}\left(U_a\frac{\partial G}{\partial N_a}-G\frac{\partial\phi}{\partial N_a}\right)\Bigg|_{y=h_a+D}dxdz = \begin{cases}\phi(\mathbf{r}') & \text{if } \mathbf{r}'\in V\\ 0 & \text{if } \mathbf{r}'\notin V\end{cases}, \tag{1}$$

where ϕ is the electrostatic potential, G is the Green function of Laplace's equation, U_b and U_a are the electrostatic potentials of the lower and upper electrodes, respectively, and the differential operators are $\partial/\partial N_b=[-h_x\partial/\partial x+\partial/\partial y-h_z\partial/\partial z]$ for $h=h_b$ and $\partial/\partial N_a=-[-h_x\partial/\partial x+\partial/\partial y-h_z\partial/\partial z]$ for $h=h_a$. Using the integral representation of the Green function[2]

$$G(\mathbf{r}-\mathbf{r}')=\frac{-1}{8\pi^2}\int_{-\infty}^{\infty}\frac{1}{k_y}\exp[-j\mathbf{k}_t\cdot(\mathbf{r}_t-\mathbf{r}_t')]\times\exp[-k_y|y-y'|]\mathrm{d}^2\mathbf{k}_t, \tag{2}$$

in (1) yields

$$\int_{-\infty}^{\infty}[(j\mathbf{k}_t\nabla h_b\pm k_y)U_b-B(\mathbf{r}_t)]\times\frac{\exp\{-j\mathbf{k}_t\cdot(\mathbf{r}_t-\mathbf{r}_t')\pm k_y[h_b(\mathbf{r}_t)-y']\}}{k_y}\mathrm{d}^2\mathbf{r}_t\mathrm{d}^2\mathbf{k}_t - \int_{-\infty}^{\infty}[(j\mathbf{k}_t\nabla h_a\pm k_y)U_a-A(\mathbf{r}_t)]\times\frac{\exp\{-j\mathbf{k}_t\cdot(\mathbf{r}_t-\mathbf{r}_t')\pm k_y[D+h_a(\mathbf{r}_t)-y']\}}{k_y}\mathrm{d}^2\mathbf{r}_t\mathrm{d}^2\mathbf{k}_t=0, \tag{3}$$

where the + sign in the exponentials is for $y'>D+(h_a)_{\max}$ and the − sign for $y'<(h_b)_{\min}$, the subscript t denotes two-dimensional vectors in the xz plane, i.e., $\mathbf{k}_t=(k_x,k_z)$ and $\mathbf{r}_t=(x,z)$, $k_y=(k_x^2+k_z^2)^{1/2}$, $\partial\phi/\partial N_b|_{y=h_b}\equiv B(x,z)$, and $\partial\phi/\partial N_a|_{y=h_a}\equiv A(x,z)$. The charge density per unit area of the transverse plane (i.e., per $dxdz$) is $\varepsilon_0 B(x,z)$ and $\varepsilon_0 A(x,z)$ for the lower and upper electrodes, respectively (ε_0 being the dielectric permittivity between the electrodes). This is a system of two equations (signs + and −) with two unknowns (A and B). We may drop from (2) the integral operator on $d^2\mathbf{k}_t$ and the factor $\exp(j\mathbf{k}_t\cdot\mathbf{r}_t')$, since both together correspond to a Fourier transform with respect to $\mathbf{r}_t'$ (recall that the Fourier transform pair is a one to one relationship). By replacing $(\nabla h_b)\exp(\pm k_y h_b)$ by $\pm\nabla\times[\exp(\pm k_y h_b)-1]/k_y$ and assuming that h_b is zero outside a large but finite square on the xz plane, we may integrate by parts the corresponding integral.[2] Using similar steps on the integral with ∇h_a we get

[a]Electronic mail: garciaa@aleph.cinstrum.unam.mx

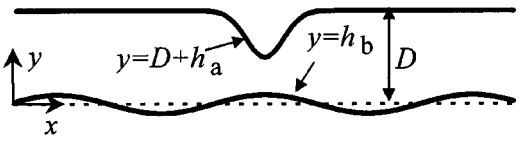

FIG. 1. Electrodes geometry. The dashed line corresponds to the mean plane of the lower profile (xz plane) which is considered rough.

$$\int_{-\infty}^{\infty} B(\mathbf{r}_t)\exp[-j\mathbf{k}_t\cdot\mathbf{r}_t \pm k_y h_b(\mathbf{r}_t)]\mathrm{d}^2\mathbf{r}_t - \exp(\pm k_y D)\int_{-\infty}^{\infty} A(\mathbf{r}_t)\exp[-j\mathbf{k}_t\cdot\mathbf{r}_t \pm k_y h_a(\mathbf{r}_t)]\mathrm{d}^2\mathbf{r}_t = \mp 2\pi k_y U_{ab}\delta(\mathbf{k}_t), \tag{4}$$

where $U_{\mathrm{ab}}=U_a-U_b$ and $\delta(\mathbf{k}_t)$ is the Dirac's delta function $\delta(k_x)\,\delta(k_z)$.

We may use PT to solve (4) in the same way as in Ref. 2. In this case, we must introduce the perturbation parameter ε (dimensions of length) on both surface profiles, i.e., we write $h_a=\varepsilon H_a$ and $h_b=\varepsilon H_b$ where functions H_a and H_b are dimensionless. Expanding A and B in a series of powers of ε (e.g., $A=A_0+A_1+A_2+\ldots=a_0+\varepsilon a_1+\varepsilon^2 a_2+\ldots$) and expanding $\exp(\pm\varepsilon k_y H)=1\pm\varepsilon k_y H+\frac{1}{2}(\varepsilon k_y H)^2\pm\ldots$ for H_a and H_b and then enforcing Eq. (4) to each order in powers of ε, yields $A_0=B_0=U_{\mathrm{ab}}/D$, and for $n\geqslant 1$,

$$\mathfrak{I}(B_n)-e^{\pm k_y D}\mathfrak{I}(A_n)+\left\{\sum_{m=1}^{n}\frac{(\pm k_y)^m}{m!}\times[\mathfrak{I}(B_{n-m}h_b^m)-e^{\pm k_y D}\mathfrak{I}(A_{n-m}h_a^m)]\right\}=0, \tag{5}$$

where $\mathfrak{I}(\ldots)$ denotes a Fourier transform (argument $\mathbf{k}_t$). Solving these two equations for $\mathfrak{I}(B_n)$ and $\mathfrak{I}(A_n)$ yields

$$\mathfrak{I}(A_n)=\sum_{m=1,3,5,..}^{n}\frac{k_y^m}{m!}\left[\frac{\mathfrak{I}(B_{n-m}h_b^m)}{\sinh(k_y D)}-\coth(k_y D)\mathfrak{I}(A_{n-m}h_a^m)\right]-\sum_{m=2,4,..}^{n}\frac{k_y^m}{m!}\mathfrak{I}(A_{n-m}h_a^m), \tag{6a}$$

and

$$\mathfrak{I}(B_n)=\sum_{m=1,3,5,..}^{n}\frac{k_y^m}{m!}\left[\coth(k_y D)\mathfrak{I}(B_{n-m}h_b^m)-\frac{\mathfrak{I}(A_{n-m}h_a^m)}{\sinh(k_y D)}\right]-\sum_{m=2,4,..}^{n}\frac{k_y^m}{m!}\mathfrak{I}(B_{n-m}h_b^m). \tag{6b}$$

The perturbative series can be evaluated iteratively from (6) starting with $A_0=B_0=U_{\mathrm{ab}}/D$.

For each order n one first finds the Fourier transform of the unknowns. Inverse Fourier transforming the results gives A_n and B_n. The solution to nth order for the surface-charge density is therefore, $\varepsilon_0(A_0+A_1+A_2+\ldots A_{\mathrm{n}})$ and $\varepsilon_0(B_0+B_1+B_2+\ldots B_{\mathrm{n}})$ for the upper and lower electrodes, respectively. The capacitance due to a section in the xz plane of the structure is calculated by integrating $\varepsilon_0 A$ or $\varepsilon_0 B$ across the corresponding area, resulting in $C=C_0+C_1+C_2+\ldots C_{\mathrm{n}}=c_0+\varepsilon c_1+\varepsilon^2 c_2+\ldots\varepsilon^{\mathrm{n}}c_{\mathrm{n}}$. Equation (6) can be calculated using FFT algorithms very efficiently. This formulation is for two-dimensional surface profiles. However, for simplicity, we will consider only one dimensional surface profile (i.e., no z dependence) in the following.

The validity of the first and second order solution was studied for simple periodic profiles.[2] In general, to deal with a large variety of interesting problems it is necessary to evaluate higher orders of PT. However, the series will in general have convergence problems. This is not difficult to see, at least in the following example. Consider a single frequency surface profile, e.g., $h_b=\varepsilon\cos(k_s x)$. For a given order n, the term $(k_y^m/m!)\mathfrak{I}(B_{n-m}h_b^m)$ in (6) evaluated at $m=n$ gives $(k_y^n\varepsilon^n/n!)\mathfrak{I}[\cos^n(k_s x)]$. When inverse Fourier transforming this term we obtain terms at multiples of the fundamental frequency k_s. The term of highest frequency is given by $2[(nk_s\varepsilon)^n/2^n n!]\cos(nk_s x)$. The coefficient of this term diverges as $n\to\infty$ for any k_{s} and ε. Thus, the perturbative series cannot converge.

The problem of convergence can be understood in part by going back to (2). The exponential inside the integral, $\exp[-k_y|y-y'|]$ decreases as k_y increases for any value of $|y-y'|$. A finite power series: $1-k_y\Delta y+(k_y\Delta y)^2/2-(k_y\Delta y)^3/6+\ldots+(-k_y\Delta y)^n/n!$, where $\Delta y\equiv|y-y'|$, is a good approximation to the exponential for $k_y\Delta y$ less than some value which depends on the number of terms in the series n. However, a truncated series diverges as $k_y\Delta y\to\infty$. Note that the integral in (2) is from $-\infty$ to ∞. Thus, one cannot approximate $\exp(-k_y\Delta y)$ by a truncated power series. Keeping n terms in the PT series would be equivalent to using a truncated series for the exponential. The problem is solved in some cases by introducing a spectral window function (SWF) and approximating $\exp(-k_y\Delta y)\cong[1-k_y\Delta y+(k_y\Delta y)^2/2-(k_y\Delta y)^3/6+\ldots+(-k_y\Delta y)^n/n!]\times W(k_y-k_{\max})$, where the SWF, W, is the step function: $W(t)=0$ for $t\leqslant 0$, and $W(t)=0$ for $t>0$. If we keep enough terms in the truncated series so that the minimum value is sufficiently close to 0 at some value $k_y=k_{\max}$, we get an accurate approximation for $-\infty<k_{\mathrm{x}}<\infty$. [Recall that $k_y=(k_{\mathrm{x}}^2)^{1/2}=|k_{\mathrm{x}}|$.] Therefore, we may introduce a spectral window function in (2) and have an accurate approximation. Keeping the SWF through (6), results in $W(k_y-k_{\max})$ multiplying both sides of (6a) and (6b). This means that, in this approximation, $\mathfrak{I}(A_n)$ and $\mathfrak{I}(B_n)$ are not defined outside $-k_{\max}<k_{\mathrm{x}}<k_{\max}$. We then choose $\mathfrak{I}(A_n)$ and $\mathfrak{I}(B_n)$ to be identically zero outside this range. In the iteration procedure, this is achieved by dropping $W(k_y-k_{\max})$ from the left-hand side of (6a) and (6b), while keeping it on the right hand side. A narrow enough SWF ''cuts'' the diverging terms. In practice we may choose $k_{\max}$ empirically by monitoring the convergence of the series.

We have tested the accuracy of the filtered PT series by comparing with direct numerical solution of the boundary integral equations (see Refs. 2 and 3). We refer to the latter calculations as exact. Up to now, we have only considered examples consisting of a gaussian tip on the upper electrode: $h_a=-\varepsilon\exp(-x^2/\sigma)$, and a simple periodic profile on the lower electrode: $h_b=\mu\cos(2\pi x/\lambda_s)$.

These examples may be used to model surface-profile imaging with a capacitive probe. In all cases we have assumed electrodes of length $L=50\,\mathrm{D}$. For the FFT calcula-

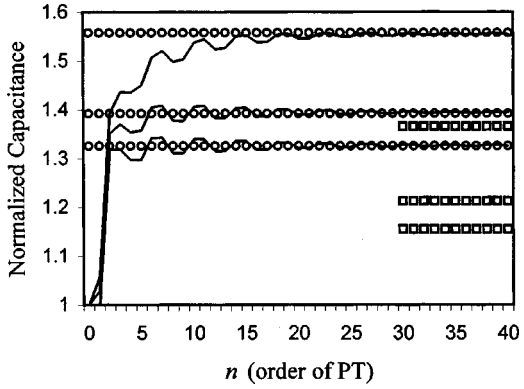

FIG. 2. The full line is for the PT results, the open circles are for exact results, and the open squares for the local height approximation. The surface parameters are $\varepsilon=0.0$, 0.2, and 0.4, $\mu=0.5$, $\lambda_s=2.5$, and $\sigma=2.0$. The SWF used $k_{\max}=3.5\times 2\pi/\lambda_s$. The larger capacitance in each case corresponds to the larger value of ε.

tions, the surface length was discretised in 256, or 512 points as needed to avoid possible aliasing problems in the FFT. We calculated 40 terms of the perturbative series in all cases. As ε or μ increase, or as λ_s or σ decrease, we need to introduce a SWF for the series to converge. Introducing the SWF allows us to calculate the capacitance for relatively large values of ε and μ, and for relatively small values of λ_s and σ. We have observed that when the series converges and it is independent to some degree of the width of the SWF, the results agree well with the exact calculations. However, beyond some limits on ε, μ, λ_s, and σ this situation is not observed and wrong results are obtained.

In Figs. 2 and 3, we show examples that are close to the limits of applicability of the filtered PT. The full lines correspond to the PT calculations, the open circles to the exact values, and the open squares to the local height approximation (LHA). Without loss of generality, we put $D=1$ and normalize all lengths with respect to D. In Fig. 2, we plot the normalized capacitance (this is the capacitance divided by the capacitance of two flat electrodes separated by D) for increasing the order of the filtered PT for $\varepsilon=0.0$, 0.2, and 0.4, $\mu=0.5$, $\lambda_s=2.5$, and $\sigma=2.0$. The normalized capacitance was calculated over the central half section of surface length (i.e, over a length of 0.5 L) The widest possible SWF corresponded to $k_{\max}=3.5\,k_s$ (where $k_s=2\pi/\lambda_s$). The figure shows that the PT series converges very close to the exact calculation (which required 512 points), while the LHA is about 50% in error. In Fig. 3 we show the convergence of the normalized capacitance for a gaussian tip of $\varepsilon=0.1$, 0.3, 0.5, and 0.7, and $\sigma=(0.1)^{1/2}$ and a flat lower electrode ($\mu=0.0$). In this case, the normalized capacitance was calculated over the central section of length 0.25 L, and we used $k_{\max}=85\times 2\pi/L$ in the SWF. As seen in the figure, the case corresponding to $\varepsilon=0.7$ does not converged. Narrowing the SWF will make the series converge but to lower values. This is an example where the filtered series fails to converge to the correct value.

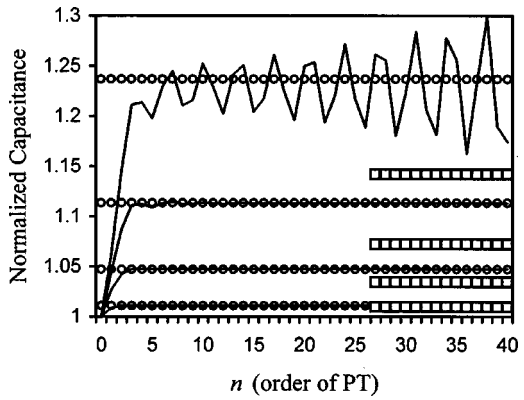

FIG. 3. The full line is for the PT results, the open circles are for exact results, and the open squares for the local height approximation. The surface profiles are a Gaussian tip with $\varepsilon=0.1$, 0.3, 0.5, and 0.7, and $\sigma=(0.1)^{1/2}$ and a flat lower electrode ($\mu=0.0$). The SWF used $k_{\max}=85\times 2\pi/\mathrm{L}$. The larger capacitance in each case corresponds to the larger value of ε.

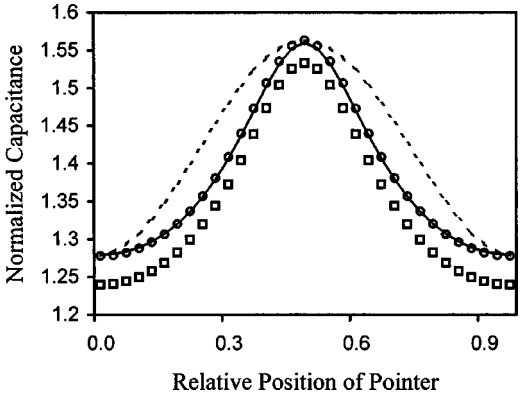

FIG. 4. The normalized capacitance as the Gaussian pointer is scanned across a period of the surface for $\lambda_s=6.25$, $\mu=0.5$, $\varepsilon=0.4$, and $\sigma=2.0$. The horizontal axis gives the position of the tip of the pointer relative to the nearest maximum of the lower cosine profile in units of λ_s .

Finally, in Fig. 4 we show the normalized capacitance as the tip is scanned laterally over a period of the cosine profile in the lower electrode. The parameters used were, $\lambda_s=6.25$, $\mu=0.5$, $\varepsilon=0.4$, and $\sigma=2.0$. The PT calculations required 40 terms, 256 points, and no SWF. To observe the fidelity of the image, we included for comparison the dashed curve which corresponds to a cosine function with equal amplitude as the exact curve. The time required to generate the PT profile in Fig. 4 was about 15 min, while the time required by the exact calculations was about 11 h, which shows a great improvement in computer time. For smoother profiles than those considered in Figs. 2–4, the filtered PT series will give correct results.

[1] C. Chang and W. Ko, in *Sensors; A Comprehensive Survey*, edited by W. Göpel, J. Hesse, and J. N. Zemel (VCH, Wienheim, 1994), Vol. 7.
[2] A. García-Valenzuela, N. C. Bruce, and D. Kouznetsov, J. Phys. D: Appl. Phys. **31**, 240 (1998).
[3] N. C. Bruce, A. García-Valenzuela, and D. Kouznetsov, J. Phys. D: Appl. Phys. **32**, 2692 (1999).
[4] Y.-P. Zhao, G.-C. Wang, T.-M. Lu, G. Palasantzas, and J. Th. M. De Hosson, Phys. Rev. B **60**, 9157 (1999).
[5] D. B. Balagurov, A. V. Klyuchnik, and Yu. E. Lozovik, Phys. Solid State **42**, 371 (2000).
[6] C. C. Williams, W. P. Hough, and S. A. Rishton, Appl. Phys. Lett. **55**, 203 (1989).
[7] S. Watanabe, K. Hane, T. Ohye, M. Ito, and T. Goto, J. Vac. Sci. Technol. B **11**, 1774 (1993).
[8] Š. Lányi, J. Török, and P. Rehurek, Rev. Sci. Instrum. **65**, 2258 (1994).
[9] K. Goto and K. Hane, Rev. Sci. Instrum. **68**, 120 (1997).